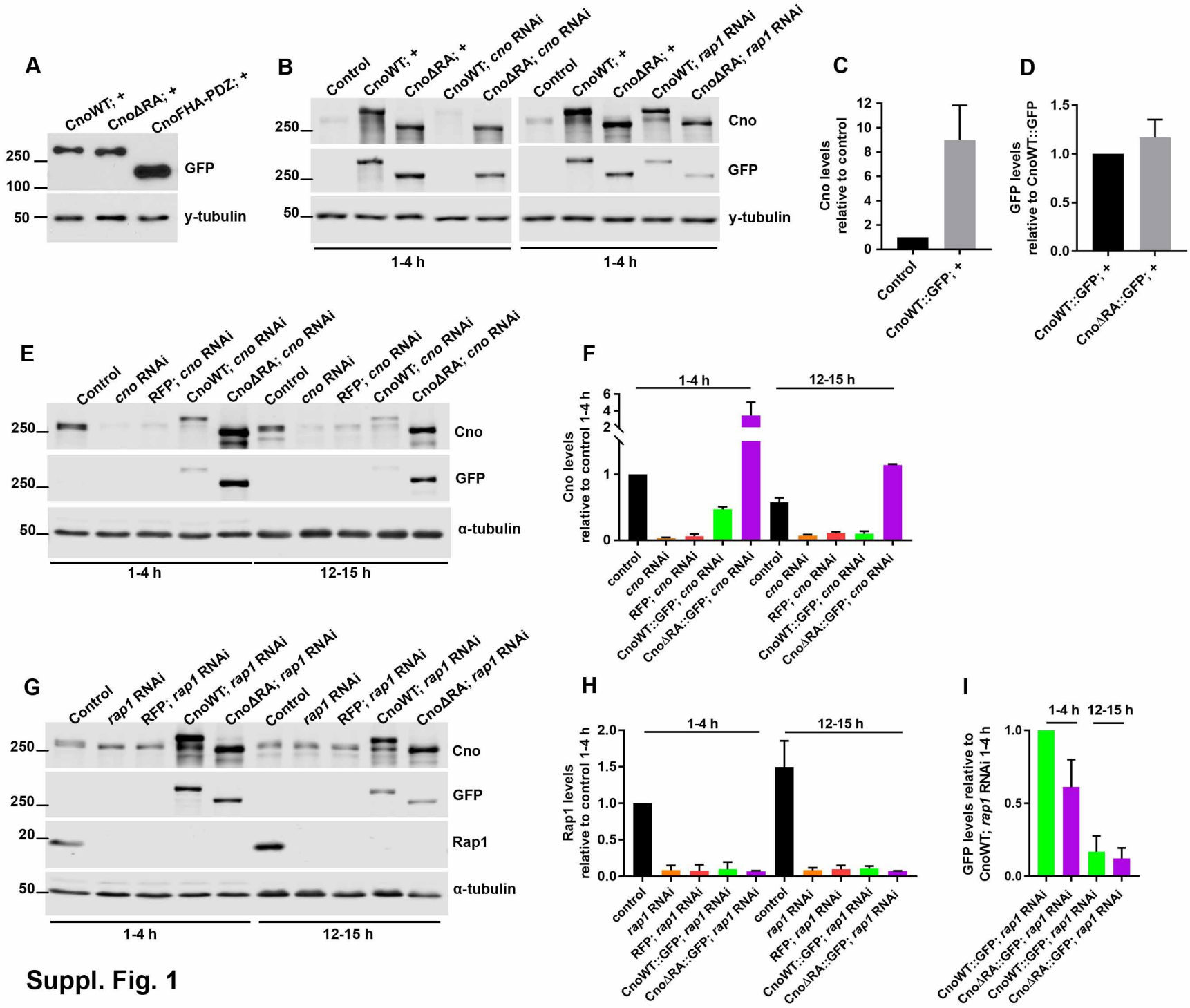

Suppl. Fig. 1

Supplementary Figure Legends

Supplementary Figure 1. Effectiveness of *cno* and *Rap1* RNAi knockdown, and expression levels of CnoWT or CnoΔRA in wildtype, Cno or Rap1-depleted backgrounds.

(A-I) Western blots assessing expression levels of endogenous Cno, endogenous Rap1, and proteins encoded by various *cno* transgenes, with accompanying quantification. In the Western blots, "control" samples are wildtype embryos, revealing endogenous levels of Cno or Rap1, and serving as negative controls for blotting with anti-GFP antibodies. Labels at the right of each blot indicate the antibody used. Times below reveal ages of embryos analysed. Note that in panels B, E, and G, assessment of levels of endogenous Cno in embryos expressing mutant or tagged versions of Cno is complicated by the fact that overexpression of CnoWT::GFP results in breakdown products similar in size to endogenous Cno, while CnoΔRA::GFP runs at an almost identical molecular weight to endogenous Cno. (A,B) Western blots showing levels of GFP-tagged Cno transgenes relative to endogenous Cno. (C) CnoWT::GFP is expressed 9-fold over endogenous Cno levels. (D) CnoWT::GFP and CnoΔRA::GFP are expressed at equivalent levels in wildtype background. (E) Western blot showing expression of GFP-tagged Cno transgenes in a *cno* RNAi background and (F) corresponding quantification of Cno levels. (G) Western blot showing expression of GFP-tagged Cno transgenes in *Rap1* RNAi background. (H) Rap1 levels are highly reduced in early embryo collections (1-4 h) and levels do not return by late embryogenesis (12-15 h). (I) CnoWT::GFP and CnoΔRA::GFP are expressed at relatively similar levels in *Rap1* RNAi background during early embryognesis, and their levels diminish by late embryogenesis.

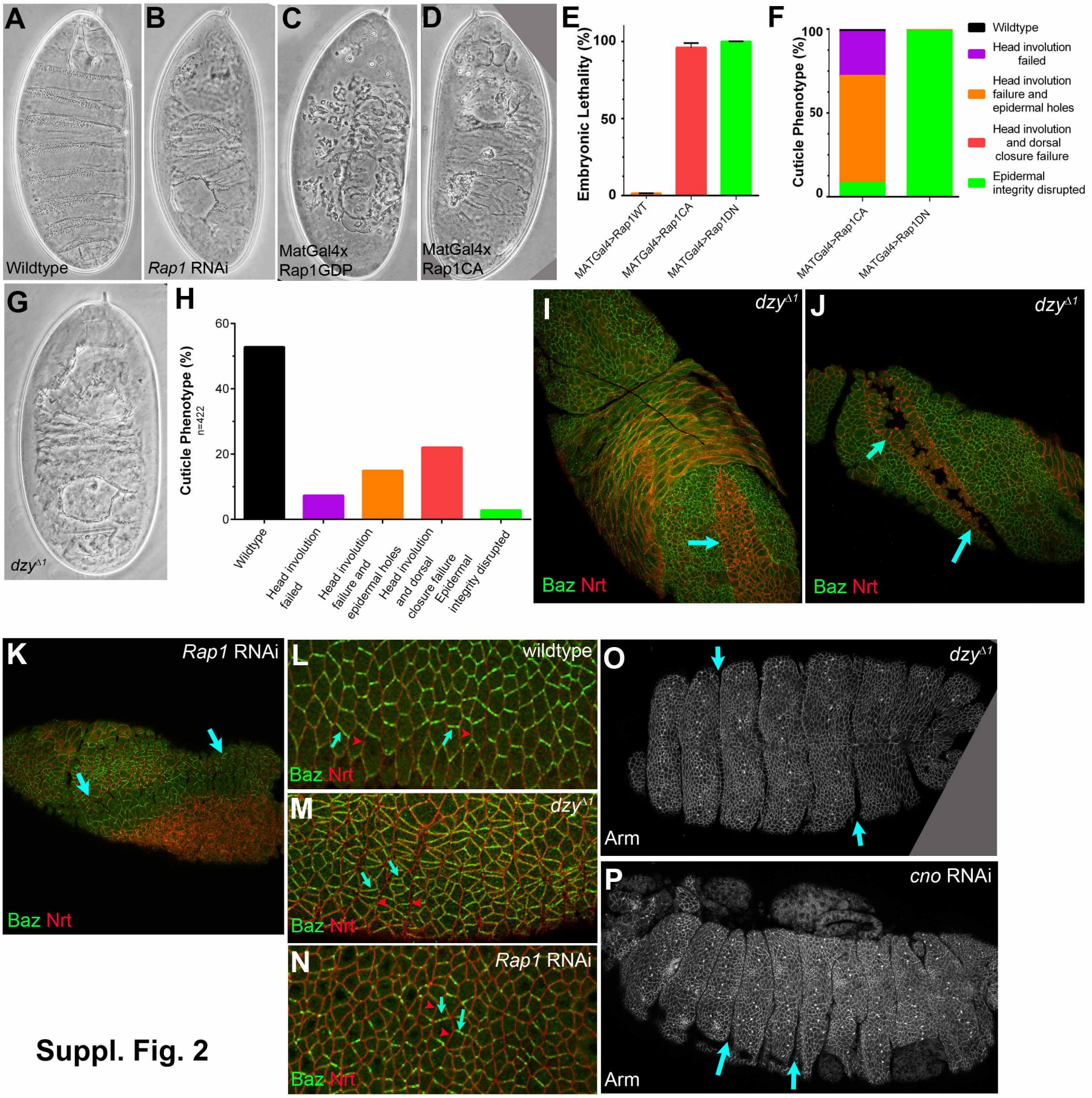
A
Wildtype
B
Rap1 RNAi
C
MatGal4x
Rap1GDP
D
MatGal4x
Rap1CA
E
Embryonic Lethality (%)
100
50
0
MATGal4>Rap1WT
MATGal4>Rap1CA
MATGal4>Rap1DN
F
Cuticle Phenotype (%)
100
50
0
MATGal4>Rap1CA
MATGal4>Rap1DN
Wildtype
Head involution failed
Head involution failure and epidermal holes
Head involution and dorsal closure failure
Epidermal integrity disrupted
G
dzyΔ1
H
Cuticle Phenotype (%)
n=422
60
40
20
0
Wildtype
Head involution failed
Head involution failure and epidermal holes
Head involution and dorsal closure failure
Epidermal integrity disrupted
I
dzyΔ1
Baz Nrt
J
dzyΔ1
Baz Nrt
K
Rap1 RNAi
Baz Nrt
L
wildtype
Baz Nrt
M
dzyΔ1
Baz Nrt
N
Rap1 RNAi
Baz Nrt
O
dzyΔ1
Arm
P
cno RNAi
Arm

Suppl. Fig. 2

Supplemental Figure 2. Phenotypes of Rap1 activity mutants and of the *dizzy* Rap1 GEF

(A-D, G) Cuticle preps, comparing effects on morphogenesis of different genotypes. (A) Wildtype. (B) *Rap1* RNAi leads to defects in head involution (red arrow) and dorsal closure and reduces epidermal integrity, as revealed by holes in the ventral cuticle (arrowhead). See Fig. 10T for quantification of these defects. (C,F) Expressing Rap1GDP leads to strong disruption of epidermal integrity--much of the cuticle is reduced to small scraps (blue arrows). (D,F) Expressing Rap1CA leads to defects in head involution (red arrow) and dorsal closure with modest effects on epidermal integrity, as revealed by holes in the ventral cuticle (arrowhead). (E) Both Rap1 activity mutants lead to highly penetrant embryonic lethality, while expressing Rap1WT has no effect. (F) Quantification of effects of Rap1 activity mutants on morphogenesis, as assessed by cuticle analysis. (G) Maternal/zygotic *dzy* mutants have defects in head involution (red arrow) and dorsal closure and reduced epidermal integrity, as revealed by holes in the ventral cuticle (arrowhead). (H) Quantification of effects of *dzy* mutants on morphogenesis, as assessed by cuticle analysis. The fraction with near wildtype cuticles include the 50% of the embryos which are zygotically-rescued. (I) *dzy* mutants fail to fully internalize their mesoderm (arrow=open ventral furrow; Spahn et al., 2012), thus resembling *cno* and *Rap1* mutants (Sawyer et al., 2009). (J, K) *dzy* mutants also have a twisted germband (J, arrows), suggesting a failure in germband extension. This is more severe than the delayed germband extension seen in *cno* mutants (Sawyer et al., 2011), but we observed a similar twisted germband phenotype with *Rap1* RNAi (K, arrows). (L-N) Lateral ectoderm, stage 8. (L) In wildtype, Baz is planar-polarized, accumulating more on dorsal-ventral (arrows) than on anterior-posterior (arrowheads) borders (Zallen and Wieschaus, 2004). (M) This planar polarity is dramatically enhanced in *dzy* mutants, with Baz lost from anterior-posterior borders (arrowheads). This mimics the effect of *cno* mutants (Sawyer et al., 2011). (N) *Rap1* RNAi embryos have a similar enhancement of Baz planar polarity, though Baz staining is already becoming more fragmented, perhaps presaging loss of epithelial integrity. (O, P) Stage 14 *dzy* mutants have abnormally deep segmental grooves (arrows), a phenotype also seen in *cno* zygotic mutants (Choi et al., 2011) or after *cno* RNAi (P).

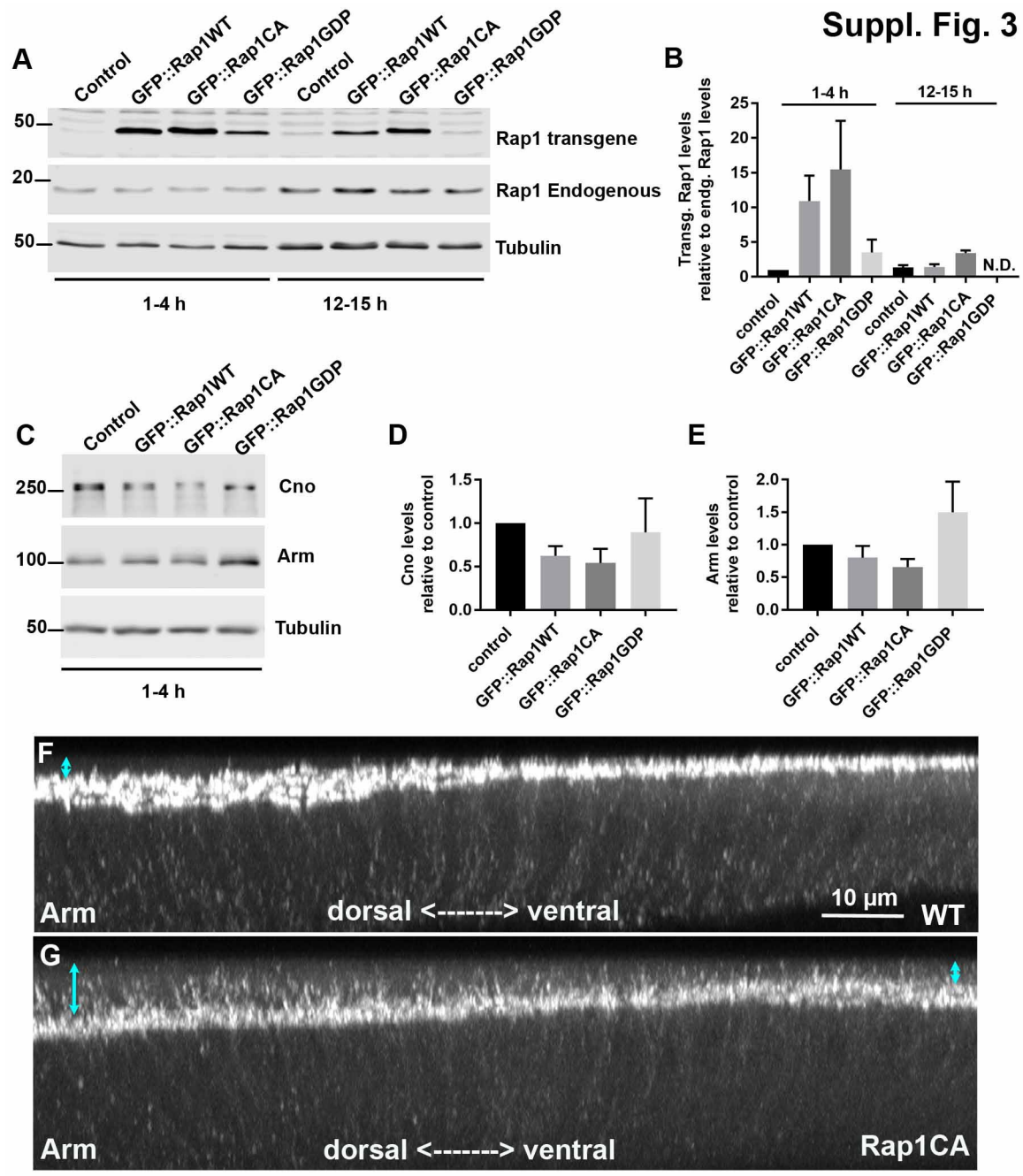

Supplementary Figure 3. Absolute levels of Rap1 activity mutants relative to endogenous Rap1. (A) Western blot assessing expression levels of endogenous Rap1 and proteins encoded by various *Rap1* transgenes. In the Western blots, "control" samples are wildtype embryos, revealing endogenous levels of Rap1, and serving as negative controls for blotting with anti-GFP antibodies. Labels at the right of each blot indicate the antibody used. Times below reveal ages of embryos analysed. (B) Corresponding quantification showing expression levels of Rap1 activity mutant protein relative to endogenous Rap1. Rap1GDP is not detectable (N.D.) in 12-15 h embryos. (C) Western blot and corresponding quantification of Cno (D) and Arm (E) levels in Rap1 activity mutants. (F,G) Maximum intensity projection of Arm localization in a cross section through the lateral ectoderm-dorsal is to the left. (F) In wildtype, apical focusing of AJs occurs earlier on the ventral side. (G) In embryos expressing Rap1CA, apical focusing of the AJs is delayed all along the dorsal-ventral axis.